SAND98-2738C

GENERATION OF CHLORIDE ACTIVE DEFECTS AT THE ALUMINUM OXIDE SURFACE FOR THE STUDY OF LOCALIZED CORROSION INITIATION

K. R. Zavadil, J.C. Barbour, F.D. Wall,
K.-A. Son, and N. Missert
Sandia National Laboratories
P.O. Box 5800, Albuquerque NM, 87185-0340

ABSTRACT

The generation of surface defects on electron cyclotron resonance (ECR) plasma derived aluminum oxide films has been studied. We find that Cl active O vacancies can be generated using electron and ion irradiation yielding surface concentrations of 3 $x10^{13}$ to $1x10^{14}$ sites·cm^{-2}. These values correspond to surface defect concentrations of 3 to 10% when compared to ordered, crystalline α-alumina. The vacancies appear to be responsible for increased surface O concentrations when immersed in water. Anodic polarization of irradiated films yields a decrease in the stable pitting potential which correlates with electron dose.

INTRODUCTION

One new approach to understanding the mechanisms of localized corrosion initiation in Al alloys is the use of Al microelectrode arrays with engineered defects incorporated at the sub-micron length scale (1). Appropriate thickness oxide layers on these surfaces represent a barrier layer with tailored or controlled defect structure incorporated. These defects should be incorporated at the passive oxide surface, within the oxide layer, and at the oxide/substrate metal interface to fully describe the potential heterogeneity present in a real material (2). Sites of strong surface adsorption of Cl are of particular interest due to the localized aggressive activity observed in chloride media (3). Oxygen vacancies generated by electron or ion impact are expected to be active to Cl sorption. Alumina has been shown to undergo O atom loss with exposure to electrons of sufficient energy and fluence (4). Our focus has been to identify whether surface vacancies generated during electron or ion stimulated desorption show activity for Cl adsorption and whether Cl populated defects sites might be carried from a vacuum environment to solution resulting in accentuated pit initiation. Due to the ability to focus energetic particles, both methods represent a possible route for generating electrochemically significant defects at the surface of microelectrodes.

EXPERIMENTAL

Al films were electron beam evaporated onto Si wafers to a thickness of ~200 nm in vacuum at a base pressure < $4x10^{-6}$ Pa. A 0.1 nm·s^{-1} deposition rate was used with a substrate temperature of 25°C resulting in 0.15 μm size grains, randomly orientated. Oxide films were grown by exposing the deposited film to an electron cyclotron resonance (ECR) plasma containing O_2 either during the final stages of film deposition or after film deposition is terminated. The former is designated a "deposited" film and the latter a "grown" film. Grown films are limited in thickness to the typical 3 nm found for air-formed oxides while deposited films can be generated to thicknesses in excess of 20

DISCLAIMER

This report was prepared as an account of work sponsored by an agency of the United States Government. Neither the United States Government nor any agency thereof, nor any of their employees, make any warranty, express or implied, or assumes any legal liability or responsibility for the accuracy, completeness, or usefulness of any information, apparatus, product, or process disclosed, or represents that its use would not infringe privately owned rights. Reference herein to any specific commercial product, process, or service by trade name, trademark, manufacturer, or otherwise does not necessarily constitute or imply its endorsement, recommendation, or favoring by the United States Government or any agency thereof. The views and opinions of authors expressed herein do not necessarily state or reflect those of the United States Government or any agency thereof.

DISCLAIMER

Portions of this document may be illegible in electronic image products. Images are produced from the best available original document.

nm. Films were stored in standard Fluoroware™ containers in a stainless steel dessicator. Adventitiously adsorbed C, collected during the storage period, was removed using O_3 exposure generated from a Hg pen lamp in the ambient atmosphere. Surfaces containing less than 1 at. % C could be generated using this pre-cleaning method. Comparison of Al^{3+} and $Al^0(2p)$ electron emission using angle resolved X-Ray Photoelectron Spectroscopy (XPS) showed no film thickening with O_3 exposure.

Surface defects were generated and electron spectroscopic analysis was conducted in a Vacuum Generators ESCALAB5 spectrometer at a base pressure of 7×10^{-8} Pa. A 300 W Mg(Kα) source was used for x-ray photoelectron spectroscopy while a rastered 3 $\mu A \cdot cm^{-2}$, 3 keV electron beam was used for Auger measurements. The same electron source was used to stimulate oxygen desorption at beam currents of 70 $\mu A \cdot cm^{-2}$ and 3 keV. Ar^+ ions of 260 eV energy at a current density of 25 $nA \cdot cm^{-2}$ were used in the ion stimulated desorption experiments. Cl sorption is produced by dosing the surface directly with 7×10^{-6} Pa Cl_2 (at 600 sec) while the surface is line-of-sight to a nude ion gauge. The ease of electron impact ionization of Cl_2 and the low recombination coefficient ensures an appreciable concentration of atomic Cl during dosing. Electrochemical measurements were made by mounting wafer coupons in a standard PAR flat cell modified to accept a Luggin capillary (1.4 mm tip diameter) within 2.8 mm of the coupon surface. A standard SCE reference electrode was used with a 50 mM NaCl electrolyte solution. An EG&G 283 potentionstat was used for potential control and current measurement using Corrware software (Scribner Assoc.). Select, short-term immersion experiments were conducted using an electrochemical cell directly coupled to the vacuum chamber (5).

RESULTS AND DISCUSSION

Cl active surface oxygen vacancies can be generated using both electron and ion irradiation. The impact of irradiation followed by Cl exposure is shown in the derivative mode Auger spectra of Figure 1. A control oxide that has only been subjected to low level electron exposure (< 1 $mC \cdot cm^{-2}$) during initial analysis shows little trace of sorbed Cl, whereas the Cl(LVV) transition at 181 eV is clearly visible for an adjoining area of the same film irradiated with 100 $mC \cdot cm^{-2}$. XPS was used to quantitatively determine the level of Cl surface coverage. We find that surface concentrations of 0.3 to 1.2×10^{14} $atoms \cdot cm^{-2}$ can be generated for both grown and deposited films. This range of values represents 2 to 10% of the idealized O surface areal density found for the O-terminated $(1\bar{1}02)$ or r-plane of sapphire. Polycrystalline α-alumina and r-plane sapphire show similar saturation levels of Cl, demonstrating that crystalline and amorphous oxides behave similarly. Ion bombardment of ECR-derived alumina films with 260 eV Ar^+ also produce saturation levels of Cl in the 1×10^{14} $atoms \cdot cm^{-2}$ range. However, implanted Ar can be detected at dose levels of 0.1 $mC \cdot cm^{-2}$ and ion transport calculations show significant levels of displacement damage, with preferential Al displacement (6). Comparison of the position of the Cl(2p) and x-ray induced Cl(LVV) transitions yields an Auger parameter of 382 eV, close to the value of 380.3 eV reported for KCl, indicating that Cl exists as an anionic species at the oxide surface. We also find that the saturation of the surface occurs rapidly, within the first 10 $mC \cdot cm^{-2}$ of electron irradiation. After electron exposure, we observe no evidence of the Al^o(LVV) transition at 68 eV indicating that large scale electron reduction and coalescence of Al islands has not occurred in the near surface of the films. The fact that surface vacancies can be generated at such low

electron doses (10^{17} electrons·cm^{-2}) when compared to the larger dose required for near surface reduction suggests that loss of O imbedded in the alumina network is the rate limiting step in the reduction mechanism (7).

Defective ECR derived alumina films retain surface Cl with exposure to atmosphere but show Cl loss when immersed in water. We find that atmospheric exposure periods of 1000 seconds reduce surface Cl by as much as 30 to 50%. This finding indicates that Cl will survive short periods of exposure prior to transfer to solution. An irradiated and Cl exposed surface shows no sign of Cl after 1000 seconds of immersion in de-ionized water. Presumably, the Cl is hydrolyzed off the surface and replaced by surface hydroxyl moieties. We find detectable increases in O/Al ratios between chlorinated and hydrated surfaces consistent with this displacement chemistry.

The character of an alumina surface environment is altered by the presence of defects when immersed in an aqueous environment. We find that films that have been irradiated but not exposed to Cl show measurable quantities of surface Cl (3 to 6×10^{13} atoms·cm^{-2}) after immersion in 50 mM NaCl and rinsing, while their non-irradiated counterparts do not. This data indicates that the electrosorption characteristics of the surface have been modified by the presence of the defects. We also find that the defective surface possesses an increased O capacity after immersion in an aqueous environment. This claim is based on Auger analysis of a single 20 nm alumina film (ECR deposited) as a function of sequential surface treatment, as shown in Figure 2. Comparison of O/Al ratios based on the O(KLL) and Al(LVV) peak-to-peak amplitudes yields a value of 3.6 for the O_3 treated surface, 2.9 for the 50 mM NaCl immersed surface, 2.1 for the electron irradiated surface, 2.4 for the post-irradiated, Cl dosed surface, and finally 4.3 for the de-ionized water immersed surface. These experiments were all conducted with 1000 second immersion periods to limit the extent of bulk film hydration. Electron irradiation produces the expected decrease in surface oxygen content through stimulated O desorption. Sorption of Cl produces a small increase in the O/Al ratio because of preferential scattering of the lower energy Al(LVV) electrons. Immersion of the irradiated film produces the largest value in surface oxygen content. The presence of increased surface O may result from an increase in surface hydroxyl density (relative to the intrinsic surface) and/or sorbed H_2O. The first step in surface aluminum atoms regaining coordination saturation after O loss might be the dissociative chemisorption of two H_2O molecules to form two surface hydroxyl species. Water sorption cannot be ruled out because it can be stable at O deficient crystalline alumina surfaces at temperatures up to 600 K (8). The consequence of an increased surface hydroxide concentration is an increase in positive surface charge ($-OH_2^+$) and an increase in compensating Cl^- sorption, assuming a basic pH of zero charge as found for crystalline, non-hydrous alumina (9).

Hydration of these ECR derived films is limited to the surface for short term exposures. We find no measurable difference in the O(1s) lineshape during the first 1000 seconds of immersion and the initial or irradiated surfaces. With continued water immersion, we find a gradual increase in the asymmetry of the O(1s) to higher binding energy, consistent with the formation of hydroxide. At immersion times of 12 hours, the hydroxide contribution contributes approximately 10% of the total O(1s) signal. Some of the films examined contained 5 at % F incorporated throughout the oxide film. (The incorporation of F into the films may result from residual F left from the buffered oxide etch used to clean the substrate wafer.) Residual F can be viewed as a marker for the hydration

process, where F would be expected to be displaced by hydroxide. Immersion of these F-containing films for 0.28, 2.5 and 12 hour shows a 0, 33 and 48% net reduction in the sub-surface F, respectively. Angle resolved XPS (ARXPS) measurements show that the F continues to be uniformly distributed through the near-surface layer after immersion. The ARXPS results highlight the lack of a discernable loss in near surface F at accentuated surface sensitivities for the first 0.28 hour. This limited F displacement from the film and the limited oxide-to-hydroxide conversion indicates that the hydration of these films is a slow process. As a result, these films represent a good model for a non-hydrous, barrier oxide on aluminum for short term experimentation.

Electron and ion irradiation appear to impact the electrochemical characteristics of these films. Figure 3 shows potentiodynamic polarization curves generated in 50 mM NaCl at 25°C at a scan rate of 167 $\mu V \cdot s^{-1}$ for a series of 3 nm thick oxide films irradiated to varying extents. We find that all of the irradiated films show an onset of stable pitting at potentials significantly more cathodic than a non-irradiated control sample. A control sample, cleaned in O_3 and subjected to low levels of electron and x-ray exposure (standard analysis) shows a pitting potential of –0.420 V (vs. SCE). In comparison, a sample exposed to a 0.014 $mC \cdot cm^{-2}$ Ar^+ ion dose and samples exposed to 65, 100 and 485 $mC \cdot cm^{-2}$ electron doses show values of -0.509, -0.549, -0.596 and -0.662 $mC \cdot cm^{-2}$, respectively. This decrease in the pitting potential correlates with the extent of irradiation and indicates that surface defects destabilize these films toward pitting. The fact that surface Cl levels saturate within the first 10 $mC \cdot cm^{-2}$ of irradiation but pitting potential continues to decrease with higher electron doses suggests that not all surface defects are populated with Cl or that the defects generated are not limited to the surface of the film. Evidence for sub-surface defect formation may be found in observed sub-surface F desorption during irradiation. We find evidence of preferential pit formation in irradiated versus non-irradiated regions using electron and optical microscopy, primarily at the high electron dose levels. The pitting is highly dispersed, uniformly distributed and follows the outline of the region of irradiation. In the absence of irradiation, ECR-derived films generally show limited numbers of isolated pits. We note that pit propagation may not be a reasonable measure of initiation and metastable event probability and that a correlation must be made through direct initiation event monitoring (1).

CONCLUSIONS

We find that surface defects in the form of O vacancies can be generated at the surface of both bulk crystalline alumina and ECR derived alumina thin films. Atomic Cl will preferentially sorb at these defects sites as an anionic species yielding surface concentrations of 3 to 10%. The threshold for generating these vacancies is substantially lower than the electron fluence required for near surface reduction of alumina, indicating that surface effects can be separated from more bulk-like defect generation processes. Ar ions can also be used to produce vacancies, but not without some degree of preferential Al cation displacement and Ar implantation within the 3 nm films studied. Sorbed Cl is hydrolyzed from the surface upon immersion in water. These defects sites show enhanced activity toward water, regardless of whether they are occupied initially by Cl, producing measurable enhancements in surface oxygen concentration. We find a decrease in the stable pitting potential with increased defect generation by electrons or ions. Evidence for preferential pitting within the irradiated regions exists, however, the continued shift in

pitting potential after saturation of surface Cl suggest that either Cl does not populate all defects or that a sub-surface mechanism is playing a role. One possible sub-surface mechanism is the loss of contaminant F through stimulated desorption.

ACKNOWLEDGMENTS

This work was performed at Sandia National Laboratories and supported by US DOE Office of Basic Energy Sciences, Metals & Ceramics Division and by Sandia Defense Programs - Research Foundations under contract DE-AC04-94AL85000.

Sandia is a multiprogram laboratory operated by Sandia Corporation, a Lockheed Martin Company, for the United States Department of Energy under contract DE-AC04-94AL85000.

REFERENCES

1. F.D. Wall, K.-A. Son, N.A. Missert, J.C. Barbour, M.A. Martinez, K.R. Zavadil, R.G. Copeland, W.R. Cieslak, R.G. Buchheit and H.S. Isaacs, this proceedings.
2. L.F. Lin, C.Y. Chao and D.D. McDonald, J. Electrochem. Soc., 128, 1194 (1981).
3. H. Bohni and H.H. Uhlig, J. Electrochem. Soc., 116, 906 (1969).
4. M.L. Knotek and P.J. Feibelman, Surf. Sci., 90, 78 (1979).
5. K.R. Zavadil, R.A. Guidotti, and W.R. Even, in Materials for Electrochemical Energy Storage and Conversion II – Batteries, Capacitors and Fuel Cells, D.S. Ginley, D.H. Doughty, B. Scrosati, T. Takamura, Z. Zhang, Vol. 496, p. 539, Materials Research Society Symposium Proceedings, Warrendale, PA (1998).
6. J.P. Biersack and L. G. Haggmark , Nucl. Inst. and Meth., 174, 257 (1980).
7. O.V. Rakhovskaya, S.S. Elovikov, E.M. Dubinina, E.S. Shakhurin and A.P. Dementjev, Surf. Sci., 274, 190 (1992).
8. M.A. Schildbach and A.V. Hamza, Surf. Sci., 282, 306 (1993).
9. W.M. Mullins and B.L. Averbach, Surf. Sci., 206, 41 (1988).

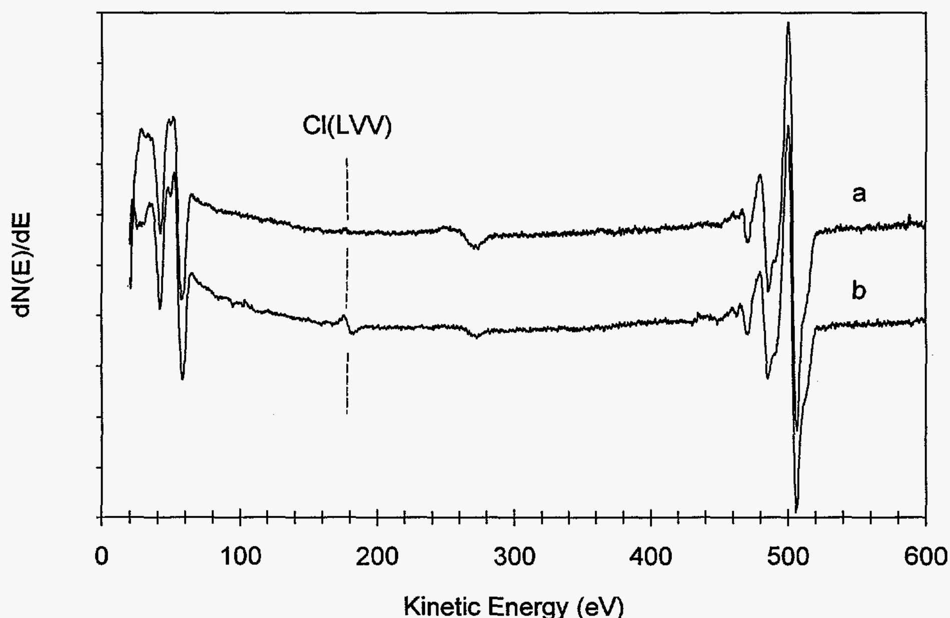

Figure 1: Selective sorption of Cl at electron-induced O vacancies on a 20 nm deposited alumina film – a) non-irradiated portion and b) irradiated portion.

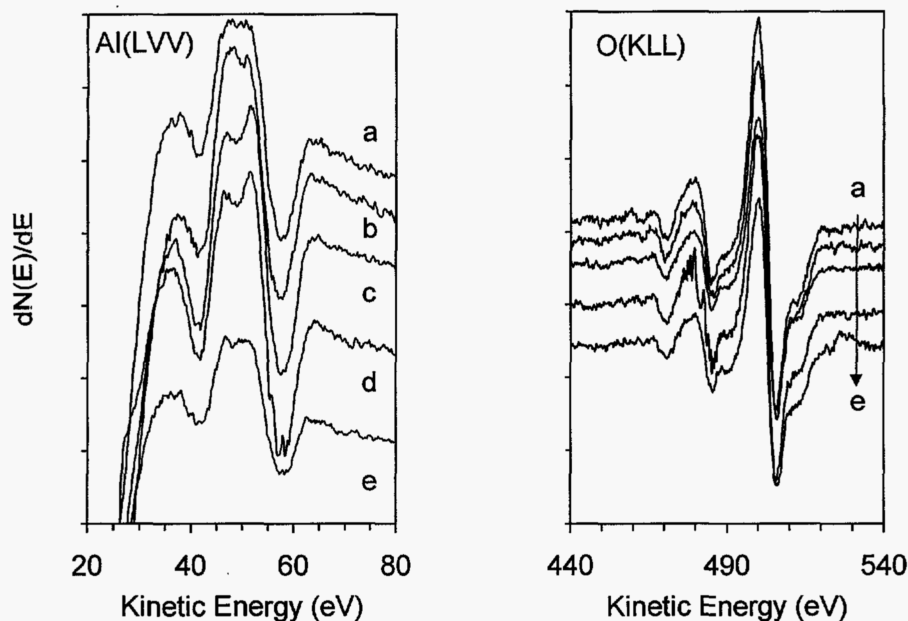

Figure 2: Variation in Al(LVV) and O(KLL) spectra with surface treatment for a 20 nm deposited alumina film: a) O_3 cleaned, b) 50 mM NaCl immersed, c) 60 mC·cm^{-2} electron irradiated, d) Cl dosed and e) de-ionized water immersed.

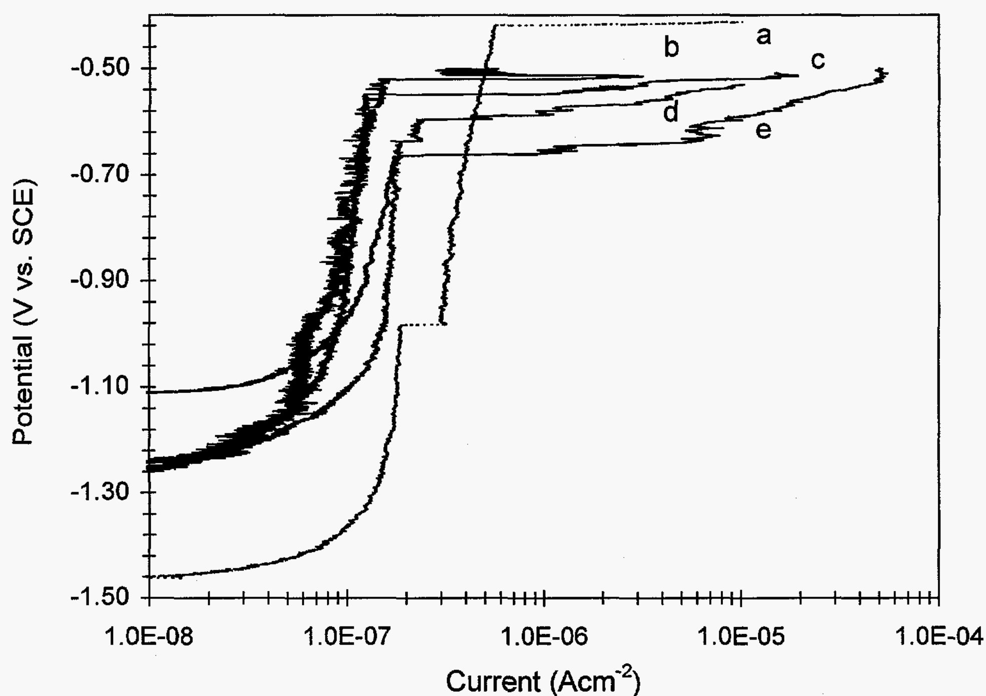

Figure 3: Anodic polarization curves for 3 nm grown oxide as a function of surface treatment: a) O_3 cleaned (----), b) 0.014 mC·cm^{-2} Ar^+ ion irradiated, c) 65 mC·cm^{-2} electron irradiated, d) 100 mC·cm^{-2} electron irradiated and e) 485 mC·cm^{-2} electron irradiated.